$Si^{28}-Al^{27}$ by combining the Al^{28} decay energy with the other Q-values. The result is a mass difference $Si^{28}-Al^{27}$ $=0.995\,702\pm0.000\,018$ MU. The mass of Si^{28} has been reported as $27.985\,810\pm0.000\,080$[11] and $27.985\,792$ $\pm0.000\,032$ MU.[12] The average of these is $27.985\,795$ $\pm0.000\,032$ MU. The mass doublet $C_2H_3-Al^{27}$ has been given as 42.35 ± 0.065 mMU.[13] Using recent values[10] for C and H, a mass of $26.989\,684\pm0.000\,070$ is found for Al^{27}. From these mass spectrographic data, one finds $Si^{28}-Al^{27}$ $0.996\,111\pm0.000\,080$ MU. The reaction mass difference $0.995\,702\pm0.000\,018$ MU is not in agreement with this and indicates that either the absolute value for Al^{27} or that for Si^{28} must be in error by about 0.4 mMU.

The most accurately measured Q-values linking Si^{28} to P^{31} and S^{32} indicate that the Si^{28} mass is consistent with the P^{31} and S^{32} masses[12] to 0.000 04 MU, which is less than the combined probable errors of the observed quantities. Similarly the mass of Si^{28} is consistent with the mass of the Ne^{20} [12] within the same limit. Thus it seems reasonable to accept the Si^{28} mass spectrographic value and reject the Al^{27} value. Using the Si^{28}, P^{31}, and S^{32} masses as standards, one can derive a mass for Al^{27} that is consistent with the known Q-values linking these isotopes.[14] Such a fit gives a value of $26.990\,140\pm0.000\,035$ for Al^{27}.

TABLE I. Calculated and observed disintegration energy of Al^{28}.

Disintegration energy (Mev)	Reaction chains and decay energies	Reference
4.657 ± 0.019	$Si^{28}(d,p)Si^{29}$ $Si^{29}(d,\alpha)Al^{27}$ $Al^{27}(d,p)Al^{28}$	[a]
4.637 ± 0.020	$Si^{28}(d,p)Si^{29}$ $Si^{29}(d,p)Si^{30}$ $Si^{30}(d,\alpha)Al^{28}$	[a]
4.647 ± 0.014	Beta endpoint 2.865 ± 0.010 Mev Gamma-ray 1.782 ± 0.010 Mev	present work

[a] See reference 9.

We are indebted to Dr. I. Feister and Miss Irene Stegun of the National Bureau of Standards for supplying the Fermi functions in advance of publication.

[11] H. E. Duckworth and R. S. Preston, Phys. Rev. **79**, 402 (1950).
[12] H. Ewald, Z. Naturforsch. **6a**, 293 (1951).
[13] S. Flügge and J. Mattauch, Physik. Z. **42**, 1 (1941).
[14] H. T. Motz, Phys. Rev. **85**, 501 (1952).

PHYSICAL REVIEW VOLUME 86, NUMBER 2 APRIL 15, 1952

Stars Initiated by High Energy Protons and Neutrons

HERBERT FISHMAN AND ALFRED MORRIS PERRY, JR.
Department of Physics, University of Rochester, Rochester, New York
(Received December 20, 1951)

Stars initiated in nuclear emulsions by 240-Mev protons and 180-Mev neutrons have been studied. Size-frequency distributions of the stars and angular distributions of prongs in various energy intervals have been obtained. Comparison with similar results obtained at different energies shows that the star size distribution is more sensitive to incident energy for protons than for neutrons.

I. INTRODUCTION

STARS in photographic emulsions have been studied by several investigators for a variety of incident particles.[1–5] In such experiments, it is hoped, from the average properties of large numbers of stars, to gain insight into the manner in which energetic nucleons interact with nuclei, and to test various nuclear models.

In the present experiment stars initiated by protons of about 240 Mev and neutrons of about 180 Mev have been examined in sensitive emulsions.

II. EXPERIMENTAL PROCEDURE

A. Protons

Ilford G-5 plates, 200, 300, and 600 microns thick were exposed to the proton beam of the 130-in. cyclotron by a method first used by Bernardini, Booth, and Lindenbaum[6] at Columbia. The plates were placed parallel to the median plane of the cyclotron, about $\frac{7}{8}$ in. above and below it, and in the neighborhood of the cyclotron radius at which $-d(\ln H)/d(\ln R)=0.2$. At this radius large vertical oscillations of the proton beam occur, and in the absence of other targets, a parallel beam of protons is spread out over the plates. In azimuth the plates were placed as far as possible from the "up-beam" edge of the dee, to reduce background caused by knock-on neutrons. Exposures were for one to two seconds with arc source and hydrogen supply turned off.

Microscopic scanning for events was done in two ways: by a systematic search over the area of the plate, and by following individual proton tracks which were selected in an unprejudiced manner near the leading edge of the plate. The latter method, while far more tedious, is much more reliable for events with few

[1] E. Gardner and V. Peterson, Phys. Rev. **75**, 364 (1949).
[2] E. Gardner, Phys. Rev. **75**, 379 (1949).
[3] L. S. Germain, Phys. Rev. **82**, 596 (1951).
[4] E. W. Titterton, Phil. Mag. **42**, 109 (1951).
[5] Bernardini, Booth, and Lindenbaum, Phys. Rev. **80**, 905 (1950); **83**, 669 (1951).
[6] S. J. Lindenbaum (private communication).

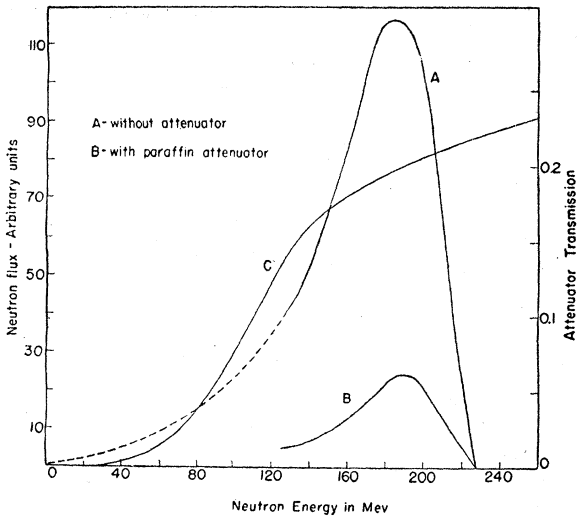

FIG. 1. Spectrum of neutrons produced by 240-Mev protons on $\frac{1}{2}$-in. Be target. Curve B shows spectrum behind 107 cm of paraffin; curve C shows the transmission of the paraffin.

prongs, and indeed is mandatory for the observation of small scatters and stoppings (in which the proton track vanishes in flight, presumably suffering a charge exchange scatter).

Star prongs were roughly classified by inspection into three groups: (1) black, including protons of about 30 Mev or less, deuterons less than 60 Mev, and all alpha-particles likely to be encountered in this experiment; (2) gray-black, including protons between 30 and 70 Mev, deuterons from 60 Mev; and (3) gray, consisting of protons above about 70 Mev. Only tracks greater than 5 microns in length were counted as prongs.

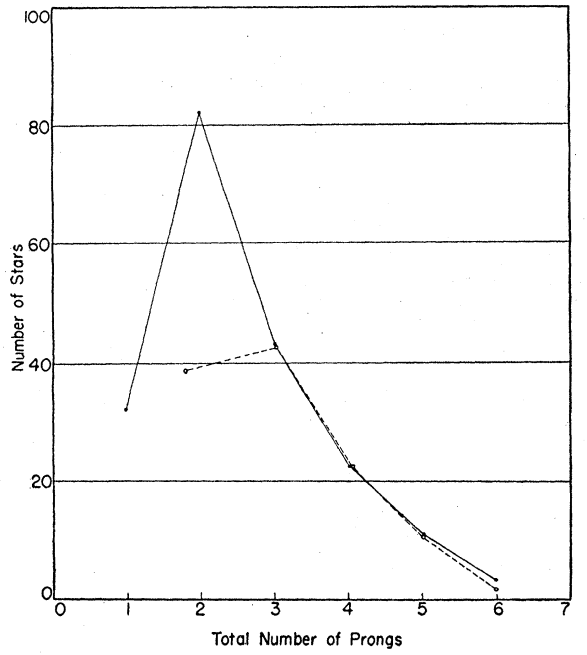

FIG. 2. Size-frequency distributions for neutron and proton stars. Solid curve: 240-Mev protons. Dashed curve: 180-Mev neutrons. Curves normalized at 3 prongs.

Criteria for judging the tracks were established partly by the ranges of a few long prongs, and partly by an empirical relation for grain density *vs* ionization, calibrated by 240-Mev protons. This relation, first brought to our attention by Dr. David Ritson, is

$$N=N_0(1-e^{-I/I_0}),$$

where N_0 is a saturation grain density, I the specific ionization of the proton, and I_0 a parameter depending on the sensitivity and development of the emulsion. The single calibration at 240 Mev is evidently not sufficient to determine both N_0 and I_0. However, a choice of $N_0=150$ grains/50μ gives a curve which matches the grain counts of a few long prongs, and which agrees quite well with a series of values $N/N_{\min}$ *vs* $I/I_{\min}$ given by Bernardini.[7] ($N_{\min}$ is the grain density of a proton with minimum ionization, $I_{\min}$.) The accuracy of energy assignments was not better than ± 10 Mev in the neighborhood of 30 Mev, or ± 20 Mev in the neighborhood of 70 Mev.

TABLE I. Number of stars *vs* total number of prongs.

Number of prongs	1	2	3	4	5	6	Total
No. of proton stars	32	82	43	23	11	3	194
No. of neutron stars	···	199	225	117	55	10	606

B. Neutrons

Neutrons were produced by interposing a $\frac{1}{2}$-in. beryllium target at $58\frac{1}{2}$-in. radius in the 240-Mev proton beam. Plates being exposed to the neutron beam were placed 29 ft away from the target, inside a concrete block-house.[8] The front wall of the block-house consists primarily of 3-ft of copper, lined with 1-ft thick concrete. In front of the block-house is a 6-ft copper collimator. As further insurance against background, the plates were surrounded by a cave of lead bricks. Placed in the neutron beam, as close as possible to the target, was a column of paraffin, 107 cm long, the effect of which was to reduce the relative intensity of low energy neutrons in the beam.

While a reliable neutron spectrum has not yet been obtained, the neutron scattering group[9] believe that their final spectrum will not differ greatly from the preliminary one shown in Fig. 1. Also shown is the spectrum of the neutrons after passing through the paraffin, obtained from the incident spectrum by the transformation,

$$N(x, E)=N(0, E)\exp-(\sigma_C N_C+\sigma_H N_H)x,$$

where $x=107$ cm and σ_C, σ_H, N_C, and N_H are the total

[7] G. Bernardini (private communication to Dr. S. W. Barnes).
[8] Clifford Swartz, Rochester thesis (1951).
[9] Guernsey, Mott, and Nelson, private communication.

neutron cross sections and numbers per cm^3 of carbon and hydrogen atoms in the paraffin.

As in the case of the proton stars, it was necessary to calibrate the plates so that the neutron star prongs could be classified in broad energy intervals, even though they left the emulsion. In place of the 240-Mev calibration point which was found convenient in the proton-star plates, reliance was placed on the grain density of one very long proton track which ended in the emulsion, and on the range-energy curve for protons in G–5 emulsion.[10,11] While the grain density of a second, somewhat shorter, track differed from the first in the range 30–55 Mev by a somewhat greater amount than would be expected from statistics, they agreed within statistics elsewhere, and it was possible to ascertain in six cases of fast star prongs ending in the emulsion that the average error in deducing the energy from the grain count was 5 Mev. As in the case of proton stars, the prongs were then classified by inspection as black, gray-black, or gray, corresponding approximately to protons below 30 Mev, between 30 and 70 Mev, or above 70 Mev. Only tracks greater than 5 microns were counted as prongs.

TABLE II. Number of stars *vs* number of black prongs.

Number of black prongs	0	1	2	3	4	5	6
No. of proton stars	24	63	47	32	19	6	3
No. of neutron stars	···	89	184	175	107	39	7

Since the incident particle is not visible in the case of neutron stars, it was not feasible to record one-pronged stars. Moreover, the two-pronged events also offered some difficulty, since it was not possible in all cases to distinguish between true neutron stars and low energy scatters. Such events were considered to be neutron stars if: (1) it was possible to discern at the vertex of the star a prong less than 5 microns in length, which was considered to be a "recoil" prong; (2) it was possible to observe a difference in grain density between the two tracks; and (3) it was possible to observe an increase in grain density along both tracks in the direction away from the star. By comparison with the proton-star plates, it has been possible to exclude from consideration the alpha-particle disintegrations of thorium, which is present in the emulsion as an impurity. Hence, we can conclude that analysis of the neutron star data should: (1) not include one-pronged stars; (2) consider two-pronged events with the reservations stated above; and (3) include all events with three or more prongs as bonafide neutron stars.

III. RESULTS

Altogether 596 neutron stars were found with a total of 1847 prongs, giving an average of 3.1 prongs per star

[10] F. H. Tenney, private communication (based on reference 11).
[11] Aaron, Hoffman, and Williams, University California Radiation Laboratory Report No. 121 (1951).

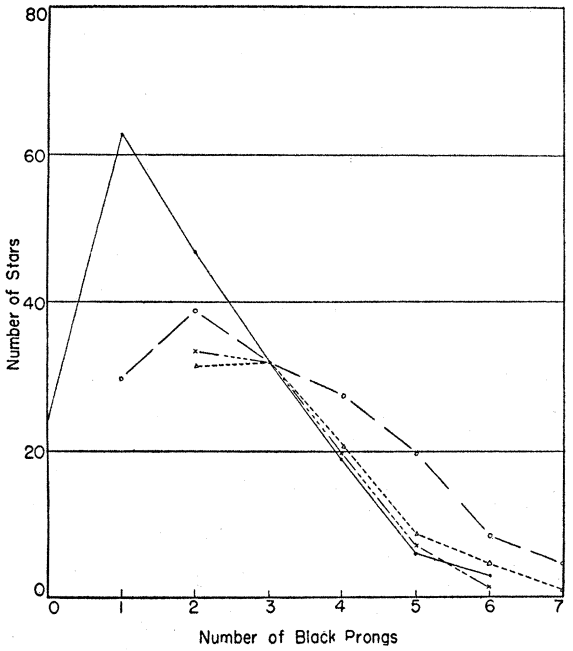

FIG. 3. Size-frequency distributions for neutron and proton stars, normalized at 3 black prongs. ○—380-Mev protons. ●—240-Mev protons. △—300-Mev neutrons. ×—180-Mev neutrons.

for stars with two or more prongs. 194 proton stars were found by the track scanning method and 321 by the area scanning method. Stars found by area scanning have been included only in the angular distribution of prongs, which we have shown to be essentially independent of star size for black and gray-black prongs, and nearly so for gray prongs.

By considering only stars with three or more prongs, we find an average of 3.6 prongs per star for neutrons and 3.7 prongs per star for protons. Size-frequency distributions for neutron and proton stars are shown

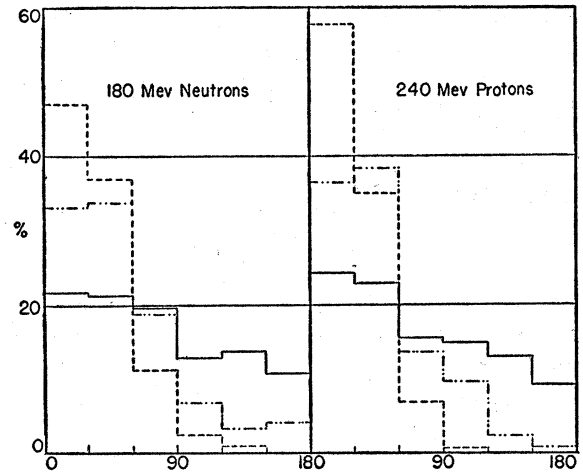

FIG. 4. Angular distributions of star prongs. Solid curves: black prongs. Dash-dotted curves: grey-black prongs. Dashed curves: grey prongs. Area under each histogram equals 100 percent.

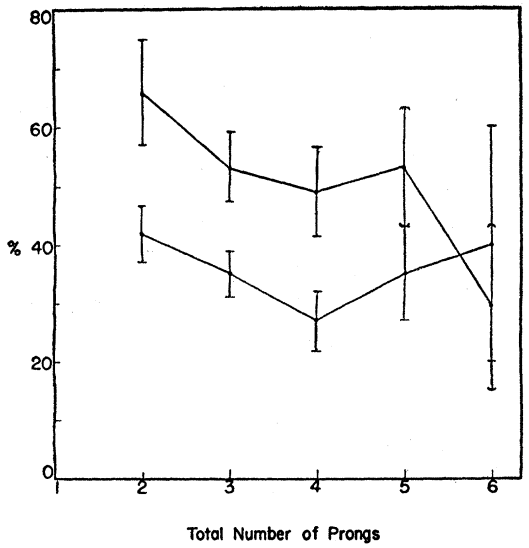

FIG. 5. Percentage of stars with N prongs having one or more gray or gray-black prongs. Upper curve: proton stars. Lower curve: neutron stars.

in Table I and in Fig. 2, in which the abscissa is the total number of prongs (excluding, of course, the incident proton). In order to compare our results with data for proton and neutron stars obtained at Columbia,[5,6] we have also plotted the number of stars against the number of black prongs as shown in Table II and in Fig. 3. The curves of Fig. 3 are normalized at three-pronged stars. The energy of the protons in the Columbia work was about 380 Mev and of the neutrons about 300 Mev.

The striking feature of this comparison is the similarity of the prong distributions for 180-Mev neutrons and for 300-Mev neutrons. The distribution obtained for 150-Mev neutrons by Titterton[4] at Harwell is also almost identical with the 180-Mev neutron curve. Furthermore, the prong distribution for 180-Mev neutron stars is essentially the same as that for 240-Mev proton stars. (While the proton data are based on a comparatively small number of stars, they are well corroborated for two or more black prongs by the area-scanning data.)

It is probably possible to understand these results in detail by making Monte Carlo calculations like those of Bernardini, Booth, and Lindenbaum.[5] This has not been done yet. The similarity in the neutron-star distributions may be a result in part of the fact that the 300-Mev neutron beam was unfiltered, while the 180- and 150-Mev neutron beams were filtered through paraffin, and therefore probably contained fewer low energy neutrons. The difference in energy dependence of the neutron- and proton-star distributions may be a result in part of the fact that the $n-p$ scattering cross section decreases with energy up to 200 Mev or above,[12] while the $p-p$ cross section is essentially independent of energy above 100 Mev.[13,14] Since protons will predominate in the first two or three generations of collisions inside the nucleus if the incident particle is a proton, while neutrons will predominate for incident neutrons, it can be seen that the effect of the energy dependence of the $n-p$ cross section is of greater consequence for neutron stars than for proton stars.

The angular distributions of star prongs in the three energy groups are shown in Fig. 4. While the distributions for neutron and proton stars are quite similar, it is seen that the gray prongs are more strongly peaked forward in the proton stars than in the neutron stars. This is probably caused in part by the difference in incident energy in the two cases, but it is also a result of the fact that the proton distribution includes stars with zero or one black prong, which contain 60 percent of all the gray prongs. (The proton distribution does not, however, include scatters resulting in a single outgoing gray track; these were not classified as stars.) For proton stars with fewer than two black prongs, the gray prongs are about 10 percent more peaked in the 0–30° interval than for proton stars with two or more black prongs.

If we consider crudely that the incident particle suffers only a single collision inside the nucleus, and that $p-p$, $p-n$, and $n-n$ collisions are equally probable at these high energies, we are led to expect three times as many visible fast prongs for incident protons as for incident neutrons. This effect is, of course, reduced by subsequent collisions inside the nucleus, but we may expect nonetheless that a higher percentage of proton than of neutron stars will exhibit fast prongs. This is confirmed by the results shown in Fig. 5.

It would doubtless be a useful extension of this work to determine the energies of the prongs more carefully in order to obtain a good energy spectrum of the prongs. It would also be desirable with the use of less sensitive emulsions to identify deuterons, alpha-particles, and heavier fragments which may be ejected as well as protons.

The authors wish to thank Dr. Sidney W. Barnes, under whose guidance the work was performed, and Dr. Robert E. Marshak, for valuable discussions. Thanks are due Mrs. Jane Button and Mr. Raymond Doughty, who assisted with the scanning.

[12] J. DeJuren and B. J. Moyer, Phys. Rev. **81**, 919 (1951).
[13] Chamberlain, Segrè, and Wiegand, Phys. Rev. **83**, 923 (1951).
[14] R. W. Birge, Phys. Rev. **80**, 490 (1950).